Molecular Dynamics Investigation of Homogeneous Nucleation in the Freezing of Selenium Hexafluoride

Prakriteswar Santikary, Kurtis E. Kinney, and Lawrence S. Bartell*

Department of Chemistry, University of Michigan, Ann Arbor, Michigan 48109

Received: April 13, 1998; In Final Form: September 24, 1998

Simulations of phase changes provide a way to investigate nucleation at a depth of supercooling so far not accessible to laboratory experiments. One helpful aspect of this regime is that deficiencies of theory are substantially magnified, helping to call attention to the weaknesses of existing treatments. In the present molecular dynamics simulations, a system of small liquid clusters of SeF_6 spontaneously froze to single body-centered cubic (bcc) crystals when cooled to 120 K. The transition was mediated by homogeneous nucleation rather than by spinodal decomposition. Its nucleation rate of 6.6×10^{35} m^{-3} s^{-1} was analyzed in both terms of classical nucleation theory (to derive the interfacial free-energy parameter) and Granasy's diffuse-interface theory (to derive the interface thickness parameter). In each case, both the classical prefactor and the Grant−Gunton (GG) prefactor were applied. Large differences between the various treatments were found. Derived interfacial free energies of 13−17 mJ/m^2 were roughly in accord with Turnbull's empirical relation. Granasy's interface thickness agreed in order of magnitude with the estimated interface correlation length of the GG prefactor and the interfacial breadth implied by a capillarywave model. Simulations provided no criterion for deciding among prefactors, but several severe flaws were found in the classical theory. Intrinsic in this theory is the attribution of bulk properties to critical nuclei and a neglect of the thickness of the interfacial region between the old phase and the new. It was found that the heat which evolved into clusters as the bcc nuclei grew was considerably less than that implied by the bulk heat of fusion. This was due to the excess interfacial enthalpy, the less efficient packing of molecules in the minute nuclei than in the bulk, or a combination of these factors. Critical nuclei contained approximately 30 molecules rather than the 5 predicted by the classical theory. Finally, the simulations revealed a transition layer around the critical nuclei of appreciable thickness.

Introduction

Although the transformation of a supercooled phase to a more stable structure has practical as well as scientific importance, knowledge of how such transformations take place on a molecular scale remains sketchy. In most liquid and gaseous systems of sufficient purity the transition is believed to take place by homogeneous nucleation. The first qualitatively correct theoretical and experimental studies of homogeneous nucleation were for the condensation of vapor.[1−3] Although they were initiated three-quarters of a century ago, only recently have experimental techniques been developed to the point at which conflicts with current theories can be assessed with accuracy.[4−6] Experimental and theoretical investigations of the kinetics of homogeneous nucleation in the freezing of liquids began later[7−12] and have not yet achieved the precision attained in condensation. Fortunately, it is now becoming feasible to carry out computer experiments to provide realistic information about spontaneous phase changes.[13−15] These molecular dynamics (MD) simulations not only yield kinetic data but also reveal what transpires on a molecular scale. No existing laboratory technique has this capacity. A number of MD simulations of transitions in monatomic systems have been carried out, the most notable involving a system of 1 million Lennard-Jones spheres[14] and a system designed to characterize critical nuclei.[15] Nucleation in these investigations was found to be in at least qualitative agreement with the classical (capillary) theory of nucleation. According to this theory, accidental fluctuations of molecules in a supercooled liquid form fleeting embryos of the more stable solid phase until, by chance, an embryo materializes that is large enough to be a "critical nucleus". A nucleus is said to be critical when the addition of one more molecule lowers the free energy of the system. The major sources of error in this theory are the attribution of bulklike properties to the critical nucleus (including the interfacial free energy at the boundary between the old and new phases) and a neglect of the thickness of the interface. Computer simulations promise to provide information about the physical properties of the nucleus and its environment. This source of information has yet to be fully exploited.

Insofar as we are aware, the present program of research is the first to investigate the dynamics of freezing in a system of polyatomic molecules free from periodic boundary conditions. This preliminary note seeks to estimate the size of critical nuclei and the magnitude of the interfacial free energy of the boundary separating the liquid from the solid phase. It also calls attention to the serious discrepancies between several alternative theoretical approaches to nucleation. One aspect of MD simulations of freezing that distinguishes them from conventional studies of nucleation in freezing is the enormously deeper supercooling in the simulations. This increases the rate sufficiently to make nucleation studies feasible with the computational power of current workstations. It also magnifies the differences between the various formulations of nucleation theory.

In subsequent papers, we will examine the structure of critical nuclei and investigate the thickness of the interface. Assumptions about this interface are one of the weakest aspects of the classical theory.

10.1021/jp981826e CCC: $15.00
Published on Web 11/19/1998

TABLE 1: Times in Heat Bath at 120 K and Nucleation Times for 138-Molecule Clusters[a]

run	time in heat bath, ps	nucleation time, ps
1	50	251
2	45	279
3	35	419
4	60	460
5	55	622
6	10	756
7	15	948

[a] Nucleation times are taken to begin when clusters emerge from the heat bath.

Our initial test system, SeF_6, was selected partly because more is known about its intermolecular potential energy function[16,17] and the molecular behavior in its condensed phases[18−21] than is the case for most simple polyatomic substances. Our choice to examine polyatomic molecular systems was also to complement our experimental studies of nucleation in supersonic jets where virtually all of our subjects have been polyatomic molecules,[20−22] including SeF_6.

Computational Details

Simulations. Molecular dynamics simulations were performed at constant energy on clusters of SeF_6 containing 138 molecules. In view of the free boundary of the clusters, the system corresponds essentially to an NPH ensemble. Runs were performed with a modified version of the program MDMPOL.[23] Time steps of 10 fs yielded good energy conservation (0.02-ppt root-mean-square deviation) and were adopted in all calculations except quenches. The subjects of the simulations were rigid molecules interacting via a potential based on pairwise-additive Lennard-Jones atom−atom functions with partial charges assigned to the atoms. The potential function, which has been described in detail elsewhere,[16,17] had been constructed to optimize crystallographic data and satisfy charges implied by the proprietary program Biograph/Polygraph.[24]

Simulations were performed on clusters instead of bulk systems to avoid the imposition of periodic boundary conditions, conditions which have been shown to interfere with phase changes unless systems are very large.[13,14] Computations for polyatomic molecules are extremely time-consuming. Even for a system as small as ours, nearly 6 months of dedicated CPU time was expended on an SGI R5000 to perform the computations described in the present paper. Therefore, in this preliminary exploration, a larger system was not feasible. For a system with only 138 molecules, a free boundary was expected to introduce fewer serious problems than a periodic boundary would. The clusters subjected to analysis were all based on a single, initially approximately spherical, cluster of SeF_6 in its low-temperature monoclinic phase. When heated, the cluster transformed to body-centered cubic (before its core melted at about 180 K. Although the cluster originally contained 150 molecules (1050 atoms), 12 evaporated when heating was continued to 220 K to ensure complete melting. The resultant 138-molecule cluster remained liquid and completely free from any crystalline seeds when cooled to 140 K. Seven (presumably sufficiently) independent configurations were generated from the original 140 K melt by running an additional 5000 time steps (every 10 fs) successively from the previous configuration. Each configuration was then cooled in steps of 10 K, spending 2000 time steps in the heat bath except at 120 K, where variable times were spent (to give a further modest differentiation between histories of different clusters), as listed in Table 1. Following the heat bath were 98 000 time steps at constant energy, except for one run in which growth was not complete after 98 000 time steps. Simulations in that run were carried out for an additional 100 000 time steps. All runs at 120 K eventually nucleated. Coordinates, velocities, quaternions, etc., for each molecule were saved every 50 steps for molecular trajectory analysis.

Recognition of bcc Aggregates. As discussed in detail in our first report on the freezing of hexafluorides,[17] a procedure based on Voronoi polyhedra[25−27] was found to be so discriminating that it could recognize molecules experiencing a bcc environment in regions far smaller than critical nuclei. When this procedure was applied, it confirmed that the liquid clusters used as starting configurations contained no seeds large enough to initiate crystallization. An analysis of Voronoi polyhedra was carried out with bcc aggregates identified via a reference set of polyhedra constructed as sketched below. It was effective in monitoring the fluctuating population of embryos of the bcc phase and the subsequent onset of nucleation and growth of crystals in the melt.

Other techniques were also applied to diagnoses of the freezing of the liquid. These included plots of configurational energies and Pawley projections,[28,29] whose meaning is sketched in the associated figure caption, and MACSPIN images[30] of the clusters. None of these alternative techniques approached the delicacy of the Voronoi analyses in detecting small aggregates with the bcc structure.

Voronoi polyhedra in a perfect bcc crystal have 14 faces, 6 with 4 edges and 8 with 6 edges. Normal bcc crystals subjected to thermal excitation and surface disorder have additional kinds of polyhedra, and Voronoi polyhedra do not apply to surface molecules. For our analysis, we generated a distribution of Voronoi polyhedra applicable to characteristic bcc clusters of 150 molecules by analyzing a cluster constructed from an ideal bcc cluster that was allowed to relax at 120 K. This provided a set of reference polyhedra for the detection of regions possessing a bcc packing of molecules. This distribution depended somewhat upon the mode of preparation of the cluster with results that are described in detail in the first paper in this series.[17] The criterion decided upon for identifying molecules associated with the bcc phase is also described. To avoid needless wordiness, we will refer to such molecules as "bcc molecules". In the results we illustrate, each configuration was quenched before being subjected to a Voronoi analysis. Linear and angular velocities for each molecule were set equal to zero after each MD step for 100 steps, and the time step was increased from 10 to 20 fs. This quenching, however, had no discernible effect on the Voronoi results.

Application of Nucleation Theory. As pointed out in the Introduction, several alternative treatments of nucleation rates have been formulated in the literature. Those applied here all express the rate of homogeneous nucleation, J, as

$$J = A \exp(-\Delta G^*/k_B T) \qquad (1)$$

where A is a prefactor and ΔG^* is the free energy of formation of a critical nucleus of the crystalline phase from the melt. Two quite different types of prefactors will be applied to the present data. One, generally considered to be the classical prefactor[7,10,31] (hereafter referred to as the "classical prefactor"), is based on molecular jump rates inferred from the rate of diffusion of molecules in a liquid; the other is the Grant−Gunton (GG) prefactor[32] based on thermal conductivity. Two different formulations of ΔG^* are also introduced. One is the classical (capillary) nucleation theory[7] (CNT) in which the free energy of isothermal formation of a spherical embryo of the solid phase

in the liquid phase depends on the radius r as

$$\Delta G(r) = 4\pi r^2 \sigma_{sl} + \frac{4}{3}\pi r^3 \Delta G_v \quad (2)$$

where ΔG_v is the (bulk) free energy of freezing per unit volume. The critical free energy ΔG^* is the extremum of $\Delta G(r)$. No explicit account of the thickness of the interface between the two phases is included in the CNT. The only consequence of the interface to enter the CNT is the excess interfacial free energy σ_{sl}. Equation 2 is given here mainly to serve as a well-known relation parallel to a less well-known relation encountered in the following. The other formulation of the free energy of formation of a critical nucleus is Granasy's diffuse-interface theory[33−36] (DIT), which explicitly takes into account the thickness of the interface between the old and new phases. Other treatments have been introduced as well, but these require more information to apply.[37,38] In analyzing our nucleation rates, we will implement both the CNT and the DIT in the calculation of ΔG^* and, in each case, compare results of applying the classical and the GG prefactors. Details of the prefactors and critical free energies of formation are given in the appendix.

Inference of Nucleation Rate from Simulations. It is taken for granted that after the time lag to achieve a steady-state generation of precritical embryos the fraction $f_1(t)$ of clusters that have not yet experienced the formation of a critical nucleus falls off according to first-order kinetics

$$f_1(t) = e^{-JV_c(t-t_0)} \quad (3)$$

where J is the rate of production of critical nuclei per unit time per unit volume of liquid, V_c is the volume of a cluster considered to be effective in nucleation, and t_0 is the initial time following the time lag. It has been found that nucleation in the hexafluorides always occurs in the interior of a cluster and never on the (disordered) surface.[21] Therefore, it is our custom to subtract the volume of the surface layer of molecules from the total volume of a cluster in order to obtain the volume V_c . We do this via the approximation

$$F = 3(4\pi/3N)^{1/3}[1 - 0.5(4\pi/3N)^{1/3}]^2 \quad (4)$$

where F is the fraction of surface molecules in a cluster of N molecules. Accordingly, the core of a 138-molecule cluster contains approximately 46 molecules. Our simulations yielded a value for the volume per molecule in the liquid of 108.7 Å^3. Obviously, an accurate determination of nucleation rate from eq 3 requires a system of many clusters. Because of the large amounts of time consumed in carrying out the simulations, our system contains only seven clusters. If errors in calculation were considered to be completely random, the uncertainty in the nucleation rate in this system would be expected to be on the order of $J/(7)^{1/2}$, or about 38%. Although this is not a small uncertainty, its effect on the derived interfacial free energy and other parameters of nucleation theory is much smaller than the imperfections in the nucleation theories themselves.

Results

The transitions from the liquid to the bcc phase can be recognized in the caloric curve $U(T)$, the time evolution of instantaneous configurational energies, the Pawley plots, the images of the clusters, and the Voronoi plots illustrated in Figures 1−5. Previous experience in this laboratory had shown that SeF_6 molecules in the cores of clusters behave very nearly the same as those in the bulk at the same temperature,[21] despite

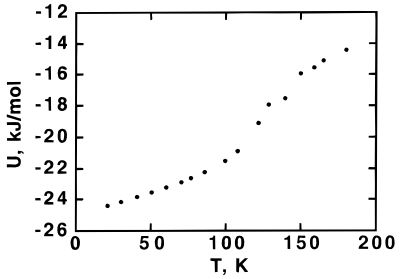

Figure 1. Configurational energy of a 138-molecule cluster (per SeF_6 molecule) as it is heated from the monoclinic phase to the liquid. An inflection in the vicinity of 130 K indicates a transition to the bcc phase shortly before melting occurs.

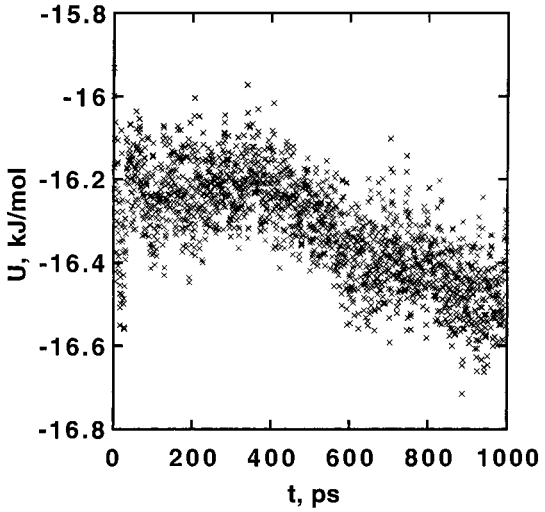

Figure 2. Evolution of configurational energy of a cluster following its emergence from the (cooling) heat bath at 120 K. A critical nucleus appeared at approximately 400 ps.

the fact that surfaces are substantially more disordered, at least for solid clusters. Therefore, in Figure 3, Pawley projections include only the core molecules. The decay of the population of liquid clusters is shown in Figure 6. A nucleation rate of 6.6 $\times$ 10^{35} m^{-3} s^{-1} was derived from the slope of this plot or, alternatively, from the mean value of $t_i - t_0$ where, from Figure 6, $t_0 \approx 210$ ps.

When the CNT is applied, it is possible to derive the interfacial free-energy parameter, σ_{sl}, corresponding to the boundary between the solid and liquid. The result obtained depends, however, upon the prefactor adopted. Alternatively, the DIT interface thickness, δ, can be determined by applying Granasy's DIT.[33−36] As is the case for σ_{sl}, the result for δ depends on the prefactor assumed to be relevant. Results for σ_{sl} and δ based on both the classical and the GG prefactors are listed in Table 2. The relations from which they were determined are outlined in the appendix.

Because all of our clusters froze at the same temperature, our results provide no information about the effect of temperature on the nucleation rate. It is possible, nevertheless, to apply nucleation theory to predict the temperature dependence. It is of some interest to do so because it graphically portrays the differences implied by the CNT and DIT and the consequences of executing analyses based on the two different prefactors. According to Granasy, the essence of the difference between the CNT and the DIT is that for the CNT one expects the parameter σ_{sl} to be approximately independent of temperature whereas for the DIT the parameter δ can be taken to be constant over a large temperature range. Note that Granasy's δ parameter, then, is essentially different from other thickness parameters

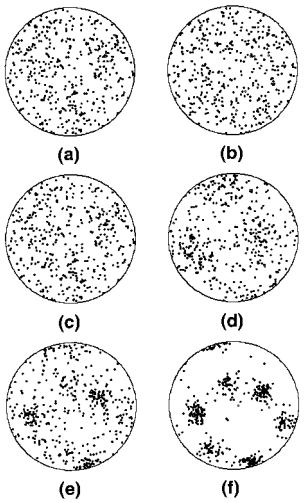

Figure 3. Pawley projections for the core molecules of a 138-molecule cluster at different stages of cooling: (a) 170 K, (b) 140 K, (c) 130 K, (d) 120 K, (e) 110 K, and (f) 80 K. These plots characterize orientations of the molecules in the cluster. They correspond to projections of Se−F bond directions on the hemisphere above the collection of molecules so that for a bcc phase three (or four) groups of dots are expected for octahedral molecules oriented with three bonds pointed upward with respect to the plane of the horizon (or two upward and two lying in the horizontal plane). For the monoclinic phase, six groups of dots are expected instead of the three for bcc. Orientational disorder in the plastically crystalline bcc phase at 120 K is very large as it is even in the bulk phase. At 110 K, the cluster begins to transform to the more ordered monoclinic phase which is clearly identifiable at 80 K.

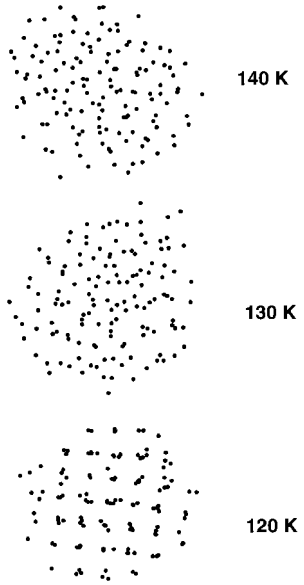

Figure 4. MACSPIN images of the centers of mass of molecules in a cluster during cooling from the liquid state to the plastically crystalline bcc phase.

such as the Tolman δ[39] and the G−G correlation length ξ which presumably decrease as the interface cools. Results for the temperature dependence of J based on Granasy's expectations are plotted in Figure 7 for both the CNT and the DIT, adjusting parameters to force nucleation rates to pass through the MD rate at 120 K. For each case, curves for both the classical and the GG prefactors are plotted.

Discussion

General Aspects of Analyses. Figures 1−5 show that the Voronoi analyses (which depend exclusively on coordinates of

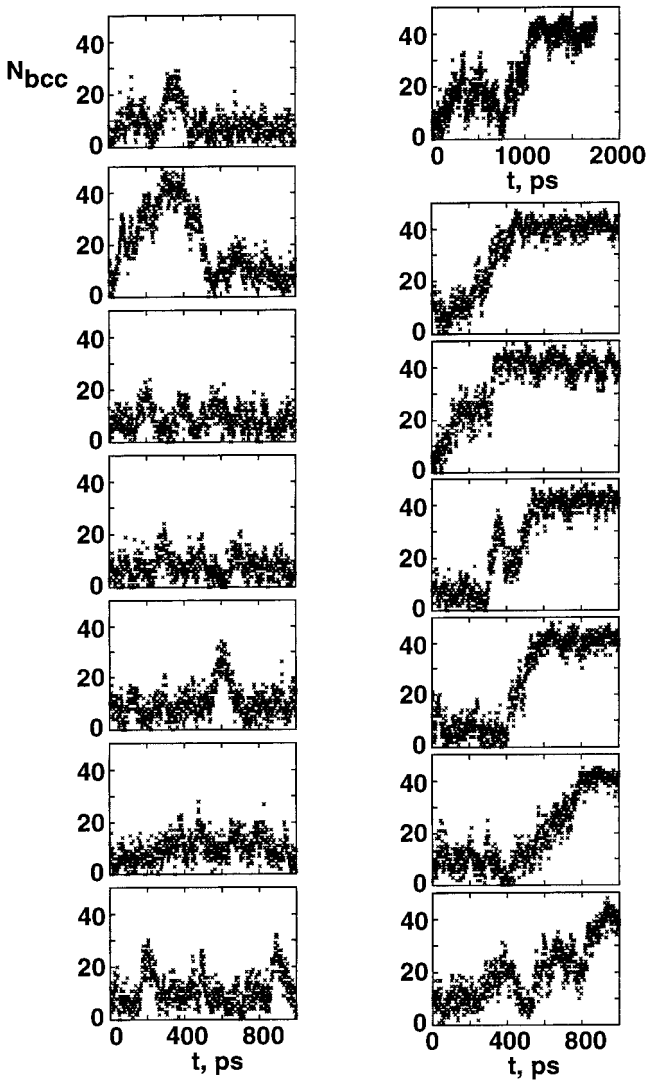

Figure 5. Histories of seven initially molten clusters of SeF_6 as exemplified by the time evolution of numbers of molecules identified as experiencing bcc environments by analyses of the Voronoi polyhedra. The left-hand column shows data at 130 K, and the right-hand column shows data later at 120 K. The fluctuating creation and disappearance of embryos is in qualitative accord with expectations of classical nucleation theory. Because Voronoi polyhedra do not apply to surface molecules, only about 46 molecules in the 138-molecule clusters are represented, but nucleation was always initiated in the interior of the clusters. Noteworthy at 130 K is the virtually complete freezing of the core of one cluster followed by its spontaneous melting, a behavior perhaps associated with a destabilization by the heat generated in the adiabatic freezing. From the distribution of nucleation times at 120 K can be derived the nucleation rate. Note that the time scales of all but the upper right-hand frame are as labeled at the base of the figures. That of the top frame at 120 K is different because the cluster took longer to freeze than the others. Points are plotted every 0.5 ps (every MD dump).

Se atoms) are much more sensitive at detecting small numbers of bcc molecules than the other diagnostic tools. They are not nearly as discriminating in differentiating between the bcc and monoclinic structures, however, as Pawley projections (which are based exclusively on molecular orientations). This is because the bcc and monoclinic structures differ principally in molecular orientations rather than in translational spacings.[40] In Figure 3, a view down a direction somewhat away from the 3-fold axis of the bcc structure that formed when the cluster froze, three patches of dots emerge which correspond to the three Se−F bonds per molecule directed upward. Orientational disorder in

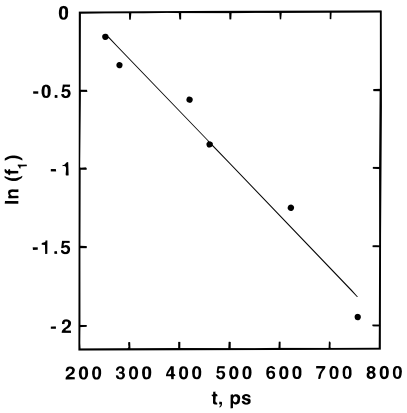

Figure 6. Plot of decay of population of liquid clusters with time.

TABLE 2: Interfacial Free-Energy Parameters (mJ/m^2) and Interface Thicknesses (Å) Derived for Clusters of SeF_6 from Nucleation Rate at 124 K[a]

parameter	Grant−Gunton prefactor	classical prefactor	ΔG^*
σ_{sl}	16.7 ± 0.15	12.9 ± 0.2	CNT[b]
δ	1.97 ± 0.02	1.57 ± 0.03	DIT[c]

[a] Uncertainties based on 40% uncertainty in nucleation rate. [b] For classical nucleation theory, see refs 7, 10, and 31. [c] For Granasy's diffuse-interface theory see refs 33−36.

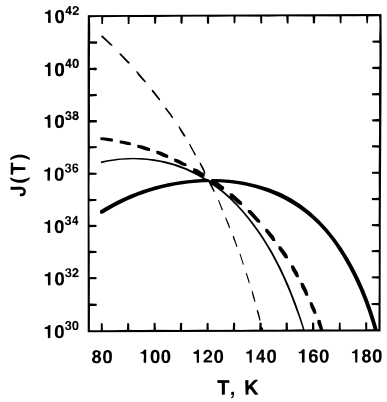

Figure 7. Calculated dependence of the rate (m^{-3} s^{-1}) of nucleation upon temperature for freezing of the 138-molecule SeF_6 clusters. Four variants of nucleation theory are invoked, each forced to pass through the rate at 124 K found in the present simulations. Serious disparities are evident. Bold curves represent classical nucleation theory, and light curves represent Granasy's diffuse-interface theory. Prefactors adopted were the classical prefactor based on molecular diffusion (solid lines) and the Grant−Gunton prefactor based on thermal conductivity (dashed lines).

the bcc structure is conspicuous, not only in the present small clusters but also in the plastically crystalline bulk. When cooled further, the three patches of spots in the Pawley plots can be seen to evolve into the six patches corresponding to the monoclinic structure. This redistribution of orientations is the consequence of one-third of the molecules in the bcc phase rotating 60° to enable the fluorines to become closely packed.[40] Pawley plots confirm that molecules in the monoclinic structure are much more ordered than those in the bcc.

All nucleation events occurring in this study led to the formation of single crystals; that is, multiple nucleations never occurred in individual clusters. Figure 4 shows that these crystals develop distinct facets.

Whether our mode of preparation of clusters with different histories is adequate to make the clusters truly independent is uncertain. Just how many time steps are required to accomplish the purpose is unclear. If molecular trajectories in clusters were too closely correlated, nucleation would presumably occur in all at nearly the same time and the rate derived would be too large. The chaotic motions of molecules makes such closely correlated trajectories unlikely in our clusters. No discernible correlation between nucleation times and the sequence of the nucleation runs was found. To within statistical error, the distribution of nucleation times (Figure 6) is that expected for independent clusters. In addition, orientations of the axes of the crystals nucleated were randomly distributed, uncorrelated with each other even though the cluster was rotationally constrained. Moreover, interfacial free energies inferred from nucleation rates via the CNT are in reasonably close correspondence with experience, according to Turnbull's relation[41] (to be discussed presently). This (weakly) corroborates the validity of the nucleation rates determined from our system of clusters.

Alternative Treatments of Nucleation. It is of some interest to note in Figure 7 the rather large difference between the predicted curves of $J(T)$ implied by the CNT and the DIT, particularly when the GG prefactor is employed. This suggests that one might be able to choose between alternative formulations of nucleation theory by carrying out temperature-dependent studies of nucleation rates. Difficulties might arise in such a study in that very long nucleation times would be encountered at temperatures substantially warmer than those of the present runs and at deeper supercoolings a nucleation directly to the monoclinic phase (ignored in Figure 7) instead of the present bcc phase might occur.[21] A different selection of hexafluorides might help to solve the latter problem. For SF_6, the difference between the bcc−monoclinic transition and the freezing point is larger.

Table 2 shows that the interfacial free energy derived when the GG prefactor is adopted is larger than that corresponding to the diffusion-based prefactor. This is because the GG prefactor is the much larger of the two, particularly at deep supercooling where it tends to rise because the interface correlation length ξ presumably shrinks (see appendix) whereas the increased viscosity at deep supercooling decreases the classical prefactor. Broughton et al. have shown that molecular jump rates do not necessarily fall off in parallel with the coefficient of diffusion in the liquid.[42,43] On the other hand, Granasy has presented evidence that for certain systems the classical prefactor applies accurately.[33−36] One possible way to discriminate between the prefactors would be to find which derived interfacial free-energy parameter is more reasonable. Unfortunately, practically nothing is known rigorously about the interfacial free energy around minute critical nuclei. What has been found is that if the CNT is applied with the classical prefactor, studies of nucleation rates at lower supercoolings yield a value for σ_{sl} in approximate agreement with Turnbull's empirical relation whereby

$$\sigma_{sl} \approx k_T \Delta \bar{H}_f / (\bar{V}^2 N_A)^{1/3} \qquad (5)$$

implying that σ_{sl} is proportional to the molar heat of fusion via a proportionality constant k_T, with $\bar{V}$ and N_A representing the molar volume and Avogadro's number, respectively. For nonmetals, k_T is approximately 0.32. It not clear whether the volume is supposed to be that of the liquid or solid or whether the heat of fusion is that at the melting point or the nucleation temperature. Inserting properties of SeF_6 into eq 5 yields values for σ_{sl} over the range of 15.3−17.4 mJ/m^2. These values are much closer to that derived using the GG prefactor than the

classical prefactor. In view of the fact that the empirical constant k_T was originally based on the classical prefactor, this gives little confidence that the GG prefactor is superior. Moreover, the heat of fusion of SeF_6 is poorly established. Different sources report results differing by a factor of 2.[44−46] Besides, only the CNT yields a value for σ_{sl}, and it is based upon the false assumption that the interfacial thickness is negligible. The DIT, which does incorporate some aspect of interface thickness, yields no independent value for σ_{sl}. It does yield a value for δ, but this does not discriminate between prefactors because the correspondence of δ to other measurable quantities is not known.

Critical Nuclei. Figure 5 gives evidence of the formation of fleeting bcc embryos. At least some of the embryos appear to become as large or larger than critical nuclei before decaying. This behavior, most evident at 130 K, may be partly due to the heat evolved when a nucleus grows, making the small crystalline aggregate unstable, however, the behavior could occur simply by chance. In future studies, we plan to remove the heat of crystallization rapidly in a heat bath, more nearly simulating nucleation in the bulk where heat flows quickly into the (more massive) surroundings. A crude estimate of the size of critical nuclei at 130 K can be made from the classical theory of nucleation according to which the size is about 30% larger than that at 120 K, where we do know the approximate size (see the following paragraph). Although our results demonstrate that the classical theory is inadequate in its estimation of the absolute size of critical nuclei, it may yield a plausible estimate of relative sizes.

Once the clusters are cooled to 120 K, the picture is somewhat clearer. Embryos smaller than about 20 molecules almost always dissolve before they can induce a concerted growth of the solid phase. Occasionally they can even reach 35 molecules and still dissipate before the cluster crystallizes. We speculate that the critical nucleus may be on the order of 25−35 bcc molecules by the Voronoi criterion. Clearly, this is a large enough fraction of the core molecules to suggest that more reliable results would be obtained from simulations on larger clusters. Nucleation theory presently indicates that the warmer the liquid, the larger the critical nuclei. Therefore, nuclei that would be critical at 120 K might not be at 130 K. For the sake of argument, we assume that critical nuclei in the 120 K runs possess about 30 molecules. When a bcc nucleus in a typical cluster emerging from the 120 K heat bath grows to 30 molecules at constant energy, the heat of crystallization raises the temperature by about 4.1 K, on average. Alternatively, if 30 molecules transform to bcc at constant energy, the temperature rises by about 4.6 K. This is larger than the first estimate because of existing embryos at steady state in the liquid at 120 K. The more appropriate of the alternatives to consider is the first. Therefore, in the tabulated results for σ_{sl} and δ we adopted 124.1 K as the temperature at nucleation.

Neither of the above temperature increases approaches the ~19° warming calculated to accompany the transformation of 30 molecules if they evolved the bulk heat of crystallization (7.1 kJ/mol[46]) to the cluster. Whether the large discrepancy is due to (a) errors in the model potential (calibration based on the heat of sublimation), (b) a large error in the bulk heat of fusion (values from 4.6 to 8.4 kJ/mol are reported in the literature[44−46]), (c) the less efficient packing of molecules in a small nucleus than in the bulk, or (d) an effect on the net heat of crystallization released because of the excess interfacial enthalpy is uncertain. Source d can be expressed, analogously to eq 2, as

$$\Delta U(r) = 4\pi r^2 E_{sl} + \frac{4}{3}\pi r^3 \Delta U_v \qquad (6)$$

where $\Delta U(r)$ represents the isothermal change in potential energy of the system when a spherical embryo of radius r of the solid phase is formed from the liquid, ΔU_v is the difference in potential energy per unit volume between the bulk phases, and E_{sl} is the interfacial excess energy per unit area. In the case of a small cluster freezing, a minor modification of eq 6 is needed to account for the change in surface energy of the whole cluster if the liquid and solid have different volumes. Because the two phases possess identical kinetic energies per mole and their volumes are small, the quantity $\Delta U(r)$ (which is readily calculated in the simulations) is essentially the difference in enthalpy on freezing, provided the Laplace pressure is not too large. How large E_{sl} may be is currently under investigation for SeF_6. In the case of the Lennard-Jones system, the effect of E_{sl} on the heat liberated when a solid nucleus grows is quite modest according to the results of ref 47 and certainly is not large enough to account for a 4-fold diminution from the bulk heat $(4/3)r^3\Delta U_v$. On the other hand, for the solid−vapor surface of the bcc phase of SeF_6, the excess surface energy E_{sv} is known.[21] For the condensation of vapor to form a 30-molecule cluster at the triple point, the heat evolved is only about one-quarter that of the bulk heat because of the effect of E_{sv}. If source c above is significant, as it probably is for small nuclei, then eqs 2 and 6 (which depend on bulk thermodynamic properties) are not rigorously applicable to the formation of small nuclei.

Báez and Clancy[15] reported a size effect on the free energy of embryo formation in their MD study of the freezing of Lennard-Jones spheres. That is, their free energies deviated from those expected from eq 2. Báez and Clancy attributed this deviation to a size effect on σ_{sl} rather than to ΔG_v via source c above, although this choice is not demanded by the data. Their choice would correspond in our case to postulating a size effect on E_{sl}, not ΔU_v.

For comparison with the evidence from the simulations, we calculate the size of critical nuclei at 124.1 K according to the classical theory. The classical result for the number of molecules in such nuclei is

$$n^* = \frac{32\pi\sigma_{sl}^3}{3v_m\Delta G_v^3} \qquad (7)$$

where v_m is the volume per molecule in the bcc phase (101.0 Å^3, according to the simulation). For consistency, it might be more logical to use the interfacial free energy based on the classical prefactor. The outcome is that n^* is very small, about 5 molecules. This smallness may be partly due to the use of the imperfectly determined experimental heat of crystallization in the computation of ΔG_v[48] or with a discrepancy between the bulk heat of crystallization and the heat modified by source c above. However, explicit in the classical theory is the relevance of the bulk heat of crystallization to the formation of nuclei. Therefore, if the use of a bulklike ΔG_v in eq 7 leads to an unphysical value for n^*, then that is a deficiency of the classical theory, not of the details of computation. In any event, it is obvious from Figure 5 that embryos as small as 5 molecules virtually always dissolve before the onset of growth of the solid. That is, the classical critical nucleus is appreciably smaller than the critical nuclei encountered in MD simulations. Of course,

the classical theory neglects the transition layer between the old and new phases. This layer might augment n^* for some apportionments of molecules to the inner and outer phases. To put things into perspective, note that the reasonable prescription of eq 4 implies that a core of 5 molecules is surrounded by a layer of about 28 molecules.

Interface Thickness. It is worthwhile to compare various estimates of the thickness of the interface with the radius of the critical nucleus. If the number of molecules in a critical nucleus were 5 as implied by the classical theory or roughly 30 as suggested by the MD simulations, then the corresponding radii would be 5.0 or 9.0 Å, respectively. Interface thicknesses, δ, are 1.6 or 2.0 Å according to Granasy's DIT via the classical or GG prefactor. The correlation length ξ (see the appendix) of the GG prefactor is approximately 1.3 Å at 124 K, according to our mode of estimation. Finally, if for the sake of comparison the capillary-wave prescription of ref 49 is applied, substituting interfacial free energy for the surface tension, nuclei with 5 or 30 molecules would have interface thicknesses $\langle\xi^2\rangle^{1/2}$ of 1.0 or 1.6 Å, respectively. The capillary-wave measure of thickness, derived for a liquid drop with surface modes excited, on average, by k_BT, has no firm foundation for crystalline nuclei, but it is of interest to note that it is of the same magnitude as δ and ξ. All of the measures of thickness are an appreciable fraction of the radius of a critical nucleus predicted by the CNT but are a more modest fraction of the size inferred from the MD simulation.

Concluding Remarks

As mentioned in the Introduction, little was known about molecular aspects of nucleation, especially in systems of polyatomic molecules, when the present research was initiated. It is now clear that the bulklike cores of the clusters examined were insufficiently large in comparison with the critical nuclei encountered to yield accurate results, and the failure to dissipate the heat of crystallization impeded the nucleation and growth of the solid phase. Nevertheless, several conclusions can be drawn from this highly preliminary study. The phase change in the molecular system did take place at least qualitatively in accordance with the theory of homogeneous nucleation and not by spinodal decomposition. Different formulations of nucleation theory at deep supercoolings are in serious disagreement with each other, for both the prefactor and the treatment of the free energy of formation of nuclei. Simulated rates of nucleation led to interfacial free energies that were qualitatively reasonable but of indeterminate physical meaning (as are all interfacial free energies derived from kinetics). Sizes of critical nuclei in the present investigation were substantially larger than these predicted by the classical theory of homogeneous nucleation. A similar conclusion about critical nuclei in monatomic systems has been published by Báez and Clancy.[15] Several measures of the thickness of the interface between the critical nucleus and the melt agreed in order of magnitude, but their precise values and their true physical significance have yet to be established. Fortunately, the profile of the interface is implicit in the MD simulations themselves, as embodied in the density and in the degree of translational and orientational crystalline order. An analysis of profiles based on these three observables is in progress and will be the subject of the next paper in this series.

Acknowledgment. This work was supported by a grant from the National Science Foundation.

Appendix. Nucleation Rate and Interfacial Free Energy

Classical Theory. According to the classical theory of homogeneous nucleation, the free-energy barrier ΔG^* to the-formation of a spherical critical nucleus which should be applied in the calculation of nucleation rate via eq 1 is

$$\Delta G^* = \frac{16\pi\sigma_{sl}^{\ 3}}{3(\Delta G_v + w')^2} \tag{A1}$$

where w' represents a correction for the work[50]

$$w' = \frac{2\sigma_l}{r_0}\left(\frac{\rho_l - \rho_s}{\rho_l}\right) \tag{A2}$$

with $2\sigma_l/r_0$ the Laplace pressure exerted by the outer liquid phase on the inner solid phase and ρ_l and ρ_s the densities of liquid and solid, respectively. The surface tension of the liquid at the temperature of interest (120 K) was obtained from Yaw's formula[51]

$$\sigma_l(T) = \sigma_l(T_1)\left(\frac{T_c - T}{T_c - T_1}\right)^n \tag{A3}$$

choosing $\sigma_l(T_l)$ to be 13.71 mJ m^{-2} at the melting point of SeF_6 (227 K) and n to be 1.2.

The free energy per unit volume, ΔG_v, was calculated from

$$\Delta G_v = \frac{-1}{\bar{V}}\int_{T_m}^{T}\Delta\bar{S}(T)\,dT \tag{A4}$$

where $\bar{V}$ is the molar volume of the solid and $\Delta\bar{S}(T)$ is the molar entropy of freezing at temperature T estimated with the aid of $\Delta C_p(T)$.

We adopt the expression of ref 31 for the classical prefactor

$$A_{cl} = 16(3/4\pi)^{1/3}(\sigma_{sl}/kT)^{1/2}D/\upsilon_m^{\ 2/3}\Delta r^2 \tag{A5}$$

where D is the coefficient of diffusion in the liquid and Δr is the molecular jump distance from the liquid to the solid taken to be $\upsilon_m^{1/3}$. A value for D was derived from the simulations for the liquid at 130 K via the relation

$$\langle[\mathbf{r}(t) - \mathbf{r}(t_0)]^2\rangle = \text{const} + 6Dt \tag{A6}$$

once the linear region of the mean-square displacement has been reached. Results were extrapolated to other temperatures by assuming an activation energy of about one-quarter the sublimation energy in accord with Ward's law.[52]

Alternatively, the GG prefactor for the system whose liquid volume is V is expressed as

$$A_{GG} = \kappa\Omega/V \tag{A7}$$

where κ is the dynamic prefactor

$$\kappa = \frac{2\lambda\bar{V}^2\sigma_{sl}T}{\Delta\bar{H}_f^{\ 2}(R^*)^3} \tag{A8}$$

with λ and R^* representing the thermal conductivity and radius of the critical nucleus (calculated here via the CNT), respectively, and Ω the dimensionless statistical prefactor

$$\frac{\Omega}{V} = \frac{2}{3\sqrt{3}}\left(\frac{\sigma_{sl}}{k_BT}\right)^{3/2}\left(\frac{R^*}{\xi}\right)^4 \tag{A9}$$

TABLE 3: Thermodynamic and Physical Properties Adopted for Analyses

quantity	value	reference
T_m, K	227	19
ΔH_f, kJ mol^{-1}	7.1	46
λ, W K^{-1} m^{-1}	$0.085-1.1\times10^{-6}(T-135)^2$	est[a]
$\bar{V}$ (liquid), m^3 mol^{-1}	$65.4_5\times10^{-6}$	this work
$\bar{V}$ (solid), m^3 mol^{-1}	$60.8_6\times10^{-6}$	this work
D, m^2 s^{-1}	$1.23\times10^{-6}\exp(-842/T)$	see appendix
ξ, m	$2.86\times10^{-10}(T/T_m)^{1.3}$	see appendix
ΔC_p, J mol^{-1} K^{-1}	$35.5-0.175T$	this work

[a] Estimated from data for SF_6. See: *Handbook of Thermal Conductivity of Liquids and Gases*; Vargaftik, N. B.; Filippov, L. P., Eds.; CRC Press: Boca Raton, 1994.

in which ξ is a "small correlation length" characterizing the thickness of the interface between the old and new phases. Oxtoby and Harrowell[53] have estimated correlation lengths for the face-centered cubic (fcc) substances argon, sodium, and lead and for the tetrahedral network of silicon. For the fcc materials, the correlation length corresponded to roughly $0.6v_m^{1/3}$ near the freezing point. For silicon, the correlation length was over twice that value. For want of better information, we adopted the fcc result because its packing of molecules is closer to that of SeF_6 than is that for silicon. Results of three other studies[54,55] suggested that the correlation length decreases with supercooling and $\approx (T/T_m)^{1.3}$.

Diffuse-Interface Theory. Granasy's[33-36] DIT of nucleation takes into account the separation between the mean surfaces at which the values of enthalpy and entropy change from the new phase to the old. The distance between the surfaces becomes the key parameter, δ, for the DIT. In the DIT, the free-energy barrier to the formation of a critical nucleus is

$$\Delta G^* = \frac{-4\pi}{3}\delta^3\Delta G_v\psi \qquad \text{(A10)}$$

where, letting $\eta = \Delta G_{fus}/\Delta H_{fus}$ and $q = (1-\eta)^{1/2}$, the quantity ψ is defined as

$$\psi = 2(1+q)\eta^{-3} - (3+2q)\eta^{-2} + \eta^{-1} \qquad \text{(A11)}$$

It is evident that δ can be derived from a measured nucleation rate by applying the DIT just as σ_{sl} can be derived by applying the CNT. No correction corresponding to w' in eq A1 has yet been incorporated into eq A10.

Physical Properties Adopted. For the above analyses to be self-consistent, they should use only quantities derived from the model potential function employed in the simulations. For the present purposes, however, it may be sufficient to use a few experimental quantities for certain properties, including the melting point and the heat of fusion for the bulk material. Thermodynamic properties adopted for application to the foregoing equations are listed in Table 3.

A few words should be said about the degree of supercooling. Insofar as the well-known depression of the freezing point of small crystals from the bulk value is understood, the supercooling of clusters should be reckoned from the *bulk* freezing point, *not* the freezing point of the cluster.[56] All of the general treatments of the freezing-point depression of which we are aware are variants of a capillary model. The chemical potential of the contents of a small drop to be used together with interfacial free energies in such treatments is that of the bulk of the pressure *outside* the drop.[57,58] Accordingly, in analyses involving the capillary theory, the quantity $\Delta G_v(T)$ required is inferred from the bulk chemical potentials of the liquid and the solid, and therefore, its computation is based on the *bulk* freezing point at which the chemical potentials are the same. To the extent that the capillary model is in error, and it is shown to be imperfect in ref 59, the computation of $\Delta G_v(T)$ calculated on this basis is uncertain.

Note added in proof: A preliminary value of T_m corresponding to our model potential function has been determined by extrapolation of melting points of clusters to infinite size. It was within 10 K of the experimental value.

References and Notes

(1) Farkas, L. *Z. Phys. Chem.* **1927**, *125*, 236.
(2) Volmer, M. *Kinetik der Phasenbildung*; Steinhoff: Leipzig, Germany, 1939.
(3) Becker, R.; Döring, W. *Ann. Phys. (Leipzig)* **1935**, *24*, 719.
(4) Schmidt, J. L. *Rev. Sci. Instrum.* **1981**, *52*, 1749.
(5) Strey, R.; Wagner, P. E.; Viisanen, Y. *J. Phys. Chem.* **1994**, *98*, 7748.
(6) Katz, J. L.; Fisk, J. A.; Rudek, M. M. In *Nucleation and Atmospheric Aerosols*; Kulmala, M., Wagner, P. E., Eds.; Pergamon: Oxford, 1996.
(7) Turnbull, D.; Fisher, J. C. *J. Chem. Phys.* **1949**, *17*, 71.
(8) Turnbull, D. *J. Chem. Phys.* **1952**, *20*, 411.
(9) Cormica, R. L.; Price, F. P.; Turnbull, D. *J. Chem. Phys.* **1962**, *37*, 1333.
(10) Buckle, E. R. *Proc. R. Soc. London, Ser. A* **1961**, *261*, 189.
(11) Bartell, L. S.; Dibble, T. S. *J. Am. Chem. Soc.* **1990**, *112*, 890.
(12) Bartell, L. S.; Dibble, T. S. *J. Phys. Chem.* **1991**, *95*, 1159.
(13) Honeycutt, J. D.; Andersen, H. C. *Chem. Phys. Lett.* **1984**, *108*, 535.
(14) Swope, W. C.; Andersen, H. C. *Phys. Rev. B* **1990**, *41*, 7042.
(15) Báez, L. A.; Clancy, P. *J. Chem. Phys.* **1995**, *102*, 8138.
(16) Kinney, K. E. Ph.D. Thesis, University of Michigan, Ann Arbor, MI, 1995.
(17) Kinney, K. E.; Xu, S.; Bartell, L. S. *J. Phys. Chem.* **1996**, *100*, 6935.
(18) Gilbert, M.; Drifford, M. In *Advances in Raman Spectroscopy*; Mathieu, J. P., Ed.; Heydon and Sons: London, 1972; Vol. 1.
(19) Virlet, J.; Rigny, P. *Chem. Phys. Lett.* **1970**, *6*, 377. Michel, J.; Drifford, M.; Rigny, P. *J. Chim. Phys. Phys.-Chim. Biol.* **1970**, *67*, 31.
(20) Dibble, T. S.; Bartell, L. S. *J. Phys. Chem.* **1992**, *96*, 8603.
(21) Bartell, L. S.; Xu, S. *J. Phys. Chem.* **1995**, *26*, 10446.
(22) Bartell, L. S. *J. Phys. Chem.* **1995**, *99*, 1080.
(23) Smith, W.; Fincham, D. *MDMPOL*; CCP5 Program Library; SERC Daresbury Laboratory: Daresbury, U.K., 1982.
(24) *Biograph/Polygraph*; Biograph Molecular Simulations Inc.: Waltham, MA, 1992.
(25) Tanemura, M.; Hiwatari, Y.; Ogawa, T.; Ogita, N.; Ueda, A. *Prog. Theor. Phys.* **1977**, *58*, 1079.
(26) Hsu, C. S.; Rahman, A. *J. Chem. Phys.* **1979**, *71*, 4974.
(27) Cape, J. N.; Finney, J. L.; Woodstock, L. V. *J. Chem. Phys.* **1981**, *75*, 2366.
(28) Boyer, L. L.; Pawley, G. S. *J. Comput. Phys.* **1988**, *78*, 405.
(29) Fuchs, A. H.; Pawley, G. S. *J. Phys. (Paris)* **1988**, *49*, 41.
(30) *MacSpin 3.01*; Abacus Concepts, Inc.; Austin, TX, 1991.
(31) Kelton, K. F.; Greer, A. L.; Thompson, C. V. *J. Chem. Phys.* **1983**, *79*, 6261.
(32) Grant, M.; Gunton, J. D. *Phys. Rev. B* **1985**, *32*, 7299.
(33) Granasy, L. *Europhys. Lett.* **1993**, *24*, 121.
(34) Granasy, L. *J. Non-Cryst. Sol.* **1994**, *162*, 301.
(35) Granasy, L. *Mater. Sci. Eng.* **1994**, *A178*, 121.
(36) Granasy, L. *J. Phys. Chem.* **1995**, *99*, 14183.
(37) Oxtoby, D. W. *Adv. Chem. Phys.* **1988**, *70*, 263; *J. Phys.: Condens. Matter* **1992**, *4*, 7627.
(38) Spaepen, F. In *Solid State Physics*; Ehrenreich, H., Turnbull, D., Eds.; Academic: London, 1994; Vol. 47, p 1.
(39) Tolman, R. *J. Chem. Phys.* **1949**, *17*, 118.
(40) Raynerd, G.; Tatlock, G. J.; Venables, J. A. *Acta Crystallogr.* **1979**, *B38*, 1896.
(41) Turnbull, D. *J. Appl. Phys.* **1950**, *21*, 1022.
(42) Broughton, J. Q.; Gilmer, G. H.; Jackson, K. A. *Phys. Rev. Lett.* **1982**, *49*, 1496.
(43) Burke, E.; Broughton, J. Q.; Gilmer, G. H. *J. Chem. Phys.* **1988**, *89*, 1030.
(44) Klemm, W.; Henkel, P. *Z. Anorg. Allg. Chem.* **1932**, *207*, 80.
(45) Yost, D. M.; Claussen, W. H. *J. Am. Chem. Soc.* **1933**, *55*, 887.
(46) *American Institute of Physics Handbook*, 2nd ed., Gray, D. E., Ed.; McGraw-Hill: New York, 1963; pp 4-208.

(47) Broughton, J. Q.; Bonissent, A.; Abraham, F. F. *J. Chem. Phys*. **1981**, *74*, 4029.

(48) Note that the source of error does not involve the *third* power of ΔG_v but only the *first* power because the determination of σ_{sl} for use in the equation for n^* came from extracting the quantity $\sigma_{sl}^3/\Delta G_v^2$ from the nucleation rate.

(49) Bartell, L. S. *Surf. Sci.* **1998**, *397*, 217.

(50) Fukuta, N. In *Lecture Notes in Physics, Atmospheric Aerosols and Nucleation;* Wagner, P. E., Vali, G., Eds.; Springer-Verlag: Berlin, 1989; p 504.

(51) Yaws, G. L. *Physical Properties: A Guide*; McGraw-Hill: New York, 1977.

(52) Ward, A. G. *Trans. Faraday Soc*. **1937**, *33*, 88.

(53) Oxtoby, D. W.; Harrowell, P. *J. Chem. Phys*. **1992**, *98*, 34.

(54) Harrowell, P.; Oxtoby, D. W. *J. Chem. Phys.* **1984**, *80*, 1639.

(55) Shen, Y. C.; Oxtoby, D. W. *J. Chem. Phys*. **1996**, *104*, 4233; *J. Chem. Phys*. **1996**, *105*, 6517.

(56) Reiss, H.; Mirabel, P.; Whetten, R. L. *J. Phys. Chem*. **1988**, *92*, 7241.

(57) Reiss, H.; Wilson, I. B. *J. Colloid Sci*. **1948**, *3*, 551.

(58) Reiss, H. *Methods of Thermodynamics*; Blaisdell Publishing Co.: New York, 1965; Chapter 11.

(59) Bartell, L. S.; Chen, J. *J. Phys. Chem*. **1992**, *926*, 8801.